

Received May 15, 2021, accepted May 25, 2021, date of publication June 3, 2021, date of current version June 10, 2021.

Digital Object Identifier 10.1109/ACCESS.2021.3085683

# Adaptive Pilot Pattern for Massive MIMO Systems

HALIMA BERGAOUI<sup>1</sup>, YOSRA MLAYEH<sup>1</sup>, AND FETHI TLILI

Innovative and Green Communications Systems Laboratory (GRESKOM), Higher School of Communication of Tunis, University of Carthage, Ariana 2083, Tunisia

Corresponding author: Halima Bergaoui (halima.bergaoui@supcom.tn)

**ABSTRACT** This work proposes a new adaptive pilot pattern used for pilot arrangement at the mobile station and a new channel estimation at the base station. It addresses the bit error rate (BER) performance optimization of wireless channel estimation in massive multiple-input multiple-output systems. First, we propose a new adaptive pilot pattern (APP) that offers a lower BER than the conventional pilot patterns. Then, we suggest a new channel estimation algorithm based on the APP. It is called the shifted APP-channel estimation (SACE). As a result, APP guarantees an optimal BER performance for the different system configurations, channel models, and carrier frequencies. It offers better BER performance than conventional pilot patterns, such as the long-term evolution (LTE) pilot pattern. Moreover, the shifted APP-based channel estimation algorithm solves the error floor caused by the usage of multiple subcarriers. It also offers a signal-to-noise ratio (SNR) improvement that reaches 17 dB at  $\text{BER} = 10^{-2}$  compared to the conventional minimum mean square error (MMSE) channel estimation.

**INDEX TERMS** Channel estimation, massive MIMO, pilot overhead, pilot pattern.

## I. INTRODUCTION

Theoretical research works usually assume a perfect channel state information (CSI) [1], [2]. Yet, in practical systems, one should consider the channel estimation and the errors that come with it. There are mainly three CSI estimation methods: blind, semi-blind, and pilot-aided [3]. First, blind estimation techniques are based on statistical channel properties [4], [5]. They are spectrally efficient. However, they suffer from imprecision and high complexity. Second, semi-blind estimation is a combination of statistical channel properties and known pilot symbols [6]. Although they cover some of the blind technique's shortcomings, they are not suitable for high mobility systems. Third, the pilot-aided channel estimation (PACE) is based on multiplexing some known pilot symbols with the transmitted data [7]. It is the most used technique for wireless systems with high mobility because of its simplicity and precision.

PACE splits into two parts. The first part is at the transmitter, where a pilot sequence is assigned to each user. Then, it is inserted in the available resources among the data following a specific pattern [8]. The second part is at the receiver. Channel coefficients that correspond to the pilots' positions are estimated using several algorithms such as least-square (LS) [9], minimum mean-square error (MMSE) [9], and

robust channel estimation [8]. Finally, they are interpolated among the unknown coefficients that correspond to the data positions. There are many interpolation algorithms [10] such as linear interpolation, second-order interpolation, low-pass interpolation, spline cubic interpolation, and time-domain interpolation. Next-generation wireless systems require the use of simple and linear algorithms [11]. Hence, in this paper, we consider the linear interpolation technique.

We can classify research works that investigate the PACE technique into three main axes. The first axis is the pilot assignment which refers to assigning a set of pilot sequences to the connected users. Its purpose is to reduce the interference between pilot sequences of users from different cells. Therefore, it helps to mitigate the pilot contamination issue [12]–[15]. The second axis is the pilot arrangement which refers to arranging a pilot sequence of a given user in the available frequency, time, and space resources. It consists of designing a pilot pattern to either enhance the spectral efficiency [16], [17] or improve the system's reliability [18]–[20]. The final axis is the channel estimation which refers to investigating the channel coefficients detection based on the received pilot signal. It aims to enhance the system's reliability [8], [9] or to reduce the computational complexity [21]. In this work, we are mainly interested in the second axis. Precisely, we are investigating the pilot pattern adaptation to enhance the system's BER performance.

The associate editor coordinating the review of this manuscript and approving it for publication was Adao Silva<sup>1</sup>.

Existing standards and systems such as 5G new radio (NR) [22], long term evolution (LTE) [23], and world-wide interoperability for microwave access (WiMax) IEEE 802.16 [24] are using fixed pilot patterns independently from the used frequency band. However, that all-in-one approach is no longer fit for the next generation of wireless systems. Each channel has its different coherence bandwidth and time where the CSI has almost a constant value. Hence, to have an accurate estimation, each channel should have its corresponding pilot pattern. Moreover, the system's configuration, such as the number of subcarriers, number of data streams, and symbol's time, affects the number of resources in each coherence time and bandwidth. Hence, each system's configuration also requires a corresponding pilot pattern.

Many works were interested in designing an adaptive pilot pattern to guarantee more flexibility and better reliability. However, they are either based on the channel sparsity [16]–[19] for frequency division duplex (FDD) systems or studied for single-input single-output (SISO) architectures [20]. There is no doubt that sparsity exists. However, not all the channels are guaranteed to be sparse. Besides, the transceiver hardware will destroy the sparsity unless a set of requirements are satisfied [25]. Consequently, technologies relying on channel sparsity are bound to disfunction for some users. As a solution, works in [26], [27] adopted the uplink channel estimation. It consists of sending orthogonal pilots from the mobile station to the base station, then exploiting the channel reciprocity to use the estimated coefficients for the downlink communication. That requires the assumption of the channel reciprocity, the usage of time division duplex (TDD), and a long enough coherence time for two-way transmission [26], [27]. Despite several solutions proposed in literature [28]–[31], FDD is not a preferred option for implementing massive MIMO [25], [32]. Therefore, this article adopts the TDD-based solution in [26], [27].

In this work, we propose a new adaptive pilot pattern (APP) for massive MIMO systems. We design it to enhance the BER performance independently of the channel, the frequency, and the system's parameters. Besides, we based it on the solution in [26], [27], so it does not depend on the channel sparsity. We also offer a theoretical analysis of the APP's impact on the channel estimation's BER performance. Finally, we suggest a new channel estimation at the base station called the shifted APP-based channel estimation (SACE). It aims to resolve the error floor issue caused in case the APP requires multiple subcarriers for one CSI matrix. To sum up, the main contributions are:

- The proposal of a new adaptive pilot pattern at the mobile station (APP).
- The suggestion of a new APP-based channel estimation at the base station.

To analyze and justify these contributions, we led the following works:

- A comparative study of the APP and the conventional fixed pilot patterns.

- A BER performance's theoretical study of the APP-based channel estimation.
- A numerical study of the APP and the SACE algorithms using MATLAB simulation.

The rest of the paper is organized as follows: Section two is an overview of the channel estimation technique and the adopted system's architecture. Then, the third section proposes a new pilot pattern, compares it to the conventional fixed pilot patterns, and discusses its BER performance. Next, the fourth section describes the SACE algorithm. Finally, the fifth section analyzes the APP and SACE performances using a numerical study and MATLAB simulations.

## II. SYSTEM OVERVIEW

This section is a general overview of the techniques and architectures used in this manuscript. First, we give an overview of the PACE channel estimation to distinguish its different features. Then, we describe the system's architecture that we are using in this work.

### A. CHANNEL ESTIMATION OVERVIEW

Channel estimation includes three main procedures: pilot arrangement, pilot assignment, and channel estimation. In this section, we are going to distinguish these different meanings.

#### 1) PILOT ARRANGEMENT

It consists of arranging the assigned pilot sequence in the available resources. In single-antenna orthogonal frequency-division multiplexing (OFDM) systems, pilots are designed in a 2-dimension-arrangement (frequency and time dimensions) following two main patterns. The first one is the bloc-type pilot arrangement [10], in which pilots are inserted in all the subcarriers of one OFDM symbol every coherence time. The second one is the comb-type pilot arrangement [33], in which pilots are inserted in one subcarrier every coherence band of all the OFDM symbols. For MIMO-OFDM systems, 3-dimension (3D) pilot patterns are needed.

#### 2) 3D PILOT PATTERN

It consists of arranging the assigned pilots in the time, frequency, and space dimensions. As a requirement, intersymbol interference should be eliminated. Therefore, the most common technique is to use orthogonal resources. One pilot is sent from a single antenna per frequency/time resource while the other antennas are silent. Consequently, one needs as many frequency/time resources as the number of transmit antennas. However, in massive MIMO downlink communication, this is very hard to achieve because of the large number of transmit antennas. Hence, several works are interested in resolving this pilot overhead problem. They are mainly divided into two approaches. The TDD-based approach continues using orthogonal pilots. However, it sends them from the mobile station to the base station. In this case, the number of pilots is proportional to the number

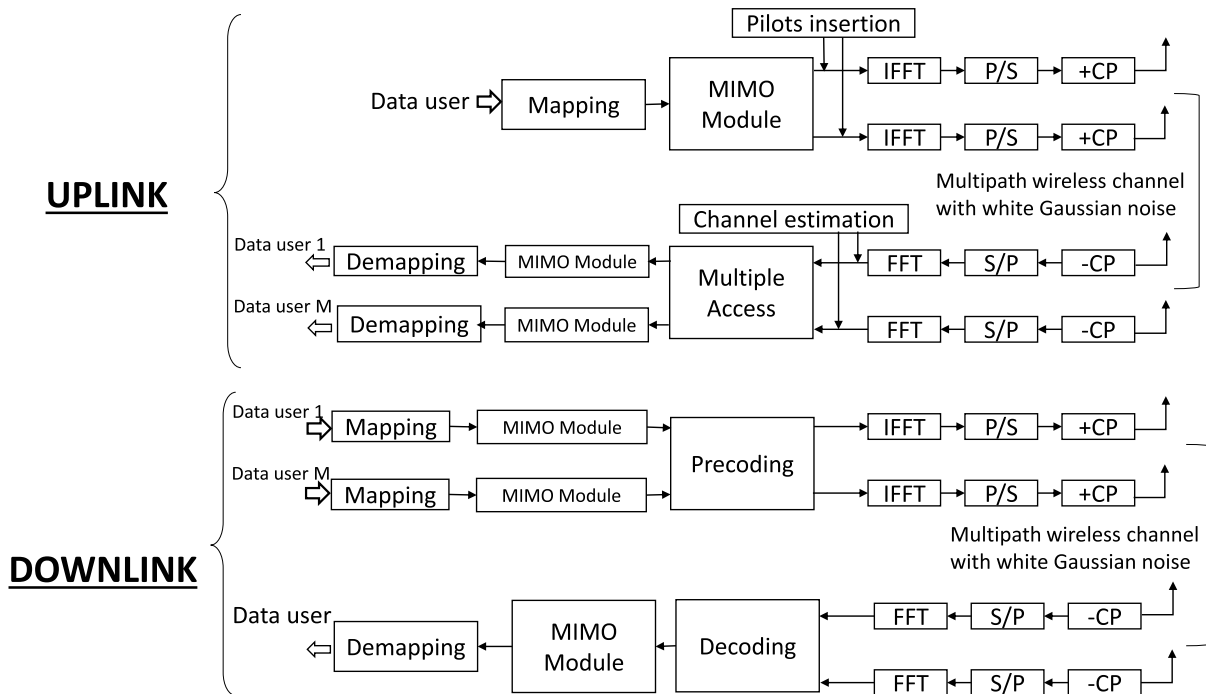


FIGURE 1. System model.

of antennas at the mobile station, which is much smaller than the number of antennas at the base station. That requires the assumption of the channel reciprocity, the usage of TDD, and a long enough coherence time for two-way transmission [26], [27]. The second approach gives up on using orthogonal pilots and is based on designing non-orthogonal pilot training to reduce the pilot overhead problem, e.g., authors in [18], [19], [28]–[31], use the compressed sensing to reduce the training and feedback overhead, but the performance relies highly on the channel’s sparsity. In this work, we are interested in the TDD-based solution in [26], [27].

### 3) PILOT ASSIGNMENT

It consists of assigning a pilot sequence to each user. Conventional pilot assignment is based on using a random pilot sequence [27], [34] and equal power allocation [35], [36] to each user. However, other works are interested in proposing different alternatives [12]– [15]. Their purpose is to reduce the interference caused by the pilot contamination in a multi-cell massive MIMO system. Pilot assignment optimization is not in the scope of this work. Hence, we are adopting a single-cell system where there is no pilot sequence’s reuse between users.

### 4) CHANNEL ESTIMATION

It consists of estimating the channel coefficients from the received pilot signal using the already known pilot sequence. Let’s take a basic example of a SISO system without an

additional noise factor. The transmitter sends a known pilot  $p$  in a given position of the available resources. Then, it goes through a channel attenuation  $h$ . The received symbol is in the form of  $y = hp$ . The channel estimation in this example following the LS algorithm consists of acquiring the value of  $h$  via dividing the received symbol  $y$  by the already known pilot  $p$ .

### B. SYSTEM’S ARCHITECTURE

This paper considers the massive MIMO-OFDM system illustrated in Fig. 1.

First, the modulated signal goes through a MIMO encoder where the MIMO technique (diversity or spatial multiplexing) is applied. Then, the pilot symbols are inserted to ensure the estimation of the channel coefficients. After that, the OFDM samples are computed via the inverse fast Fourier transform (IFFT) and a cyclic prefix is appended. In the next stage, the signal goes through a multi-path channel with additional white Gaussian noise. The received signal in the  $k^{th}$  antenna corresponding to the data’s time and frequency slots is given by (1).

$$y_k = \sum_{i=1}^{N_t} h_{k,i}(f, t)x_i(f, t) + n_k, \tag{1}$$

where  $y_k$  is the received signal of the  $k^{th}$  receive antenna,  $h_{k,i}(f, t)$  is the channel coefficient of the  $k^{th}$  receive antenna and the  $i^{th}$  transmit antenna corresponding to the  $f^{th}$  sub-carrier and the  $t^{th}$  time slot. Moreover,  $x_i(f, t)$  is the

symbol transmitted from the  $i^{th}$  antenna corresponding to the  $f^{th}$  subcarrier and the  $t^{th}$  time slot. Finally,  $n_k$  is the white Gaussian noise.

Based on the received signal, the base station estimates the channel matrix of each user. Then, it uses it to ensure the downlink communication. This paper proposes the pilot pattern mapping on uplink communication and analyzes its performances after being used for downlink communication.

### III. NEW ADAPTIVE PILOT PATTERN

This section proposes a new adaptive pilot pattern that is independent of the channel model and the system's parameters called APP. First, APP is explained. Then, it is compared to the conventional fixed pilot patterns. Finally, its BER's performances are analyzed.

#### A. ADAPTIVE PILOT PATTERN

APP is a 3D pilot pattern design that is mapped in the uplink communication. It consists of sending orthogonal pilot sequences every time/frequency coherence bloc using the algorithm Alg.1.

#### Algorithm 1 APP Mapping Algorithm

- 1: **Input:**  $B_s$  : bandwidth;  $T_s$  : number of subcarriers;  $\tau$ : delay spread;  $N_r$ : antennas number;  $p$ : sequence of known pilots
- 2: **Output:**  $P(a_r, f, t)$  : mapping grid
- 3: calculate the coherence bandwidth  $B_c$
- 4: calculate the coherence time  $T_c$
- 5: calculate the best frequency spacing  $\delta_f = \left\lfloor \frac{B_c}{B_s} \right\rfloor$
- 6: calculate the best time spacing  $\delta_t = \left\lfloor \frac{T_c}{T_s} \right\rfloor$
- 7: calculate  $\left\lfloor \frac{N_r}{\delta_t} \right\rfloor + r$
- 8: extract the number of subcarriers to be used  $N_{sc} = \left\lfloor \frac{N_r}{\delta_r} \right\rfloor$
- 9: extract the time slots number in the last subcarrier  $N_t = r$
- 10: **for** each cluster of  $\delta_t$  time slots and  $\delta_f$  subcarriers **do**
- 11:     start the mapping with the first antenna  $a_r \leftarrow 1$
- 12:     **while**  $f \leq N_{sc}$  **do**
- 13:         **while**  $t \leq \delta_t$  **do**
- 14:              $P(a_r, f, t) \leftarrow p(a_r)$
- 15:              $a_r = a_r + 1$
- 16:         **end while**
- 17:     **end while**
- 18:     **if**  $r > 0$  **then**
- 19:         **while**  $t \leq r$  **do**
- 20:              $P(a_r, N_{sc} + 1, t) \leftarrow p(a_r)$
- 21:              $a_r = a_r + 1$
- 22:         **end while**
- 23:     **end if**
- 24: **end for**

Note that  $A(x_1, \dots, x_n)$  defines a matrix  $A$  with  $x_i$  is the index of the  $i^{th}$  dimension and  $\left\lfloor \frac{a}{b} \right\rfloor$  is the greatest integer less than or equal to the result of the fraction between  $a$  and  $b$ .

To guarantee a reliable BER performance, the CSI should be constant during the channel estimation procedure. Therefore, the APP mapping starts by analyzing the channel model. First, it computes the coherence bandwidth  $B_c$  (2) and the coherence time  $T_c$  (3) [37], where  $\lambda$  is the wavelength,  $\tau$  is the root mean square (RMS) delay spread, and  $v$  is the mobility speed.

$$B_c = \frac{1}{5\tau} \tag{2}$$

$$T_c = \frac{9\lambda}{16\pi v} \tag{3}$$

Then, it clusters the physical resources into blocs of coherence bandwidth and time with the size of  $\delta_t \times \delta_f$  (defined in expressions (4) and (5)) frequency/time resources such as:

$$\delta_f = \left\lfloor \frac{B_c}{B_s} \right\rfloor \tag{4}$$

$$\delta_t = \left\lfloor \frac{T_c}{T_s} \right\rfloor \tag{5}$$

After that, pilots are mapped in a 3D dimension vector  $P(a_r, f, t)$  for each time/frequency coherence bloc, with  $a_r$  represents the known pilot's space dimension index i.e. the emitting antenna at the mobile station,  $f$  is the frequency dimension's index i.e. the pilot's subcarrier, and  $t$  is the time dimension's index i.e. the pilot's OFDM symbol's index. For a given subcarrier, each antenna transmits its pilot in a different time slot. If the number of time slots in the coherence time is lower than the number of antennas, then the remaining pilots are sent in the same positions of the next subcarrier from the same coherence bandwidth and so on.

#### B. COMPARISON WITH CONVENTIONAL PILOT PATTERNS

This section offers a comparison between the APP and the conventional fixed pilot patterns like LTE and WIMAX pilot patterns. It is done in terms of BER, pilot overhead, system flexibility, and complexity. The summary of this comparison is given in Table 1.

TABLE 1. Comparison between APP and conventional fixed pilot patterns.

<b>BER</b>	APP offers better or equal BER performance than conventional pilot patterns
<b>Pilot overhead</b>	APP offers a better or equal pilot overhead performance in case it has similar BER performance as the fixed pilot patterns. Fixed pilot patterns can offer better pilot overhead performance at the cost of a higher BER
<b>Flexibility</b>	APP is more flexible than conventional pilot patterns
<b>Complexity</b>	APP is more complex than conventional pilot patterns

Conventional pilot patterns have fixed clusters of frequency/time resources in which the pilot symbols are reinserted to estimate a new CSI matrix. For example, the LTE pilot pattern has a fixed cluster of 6 subcarriers and 4 time slots. WIMAX IEEE 802.16e has a fixed cluster of 5 subcarriers and 4 time slots. In this work, we are referring to this cluster as the conventional pilot pattern cluster.

To compare the APP and the conventional fixed pilot patterns BER performance, two use cases should be investigated. The first use case is when the system's channel is constant over a larger bandwidth or time period than a conventional pilot pattern cluster. In this case, the APP and the conventional fixed pilot pattern both give similar BER performances since the CSI is accurate for both of them. The second use case is when the channel is variable over the conventional pilot pattern cluster. In this case, the fixed pilot pattern can no longer guarantee an accurate CSI because the channel changed during the estimation of the same channel matrix. Therefore, the APP offers a better BER performance since it takes into consideration the channel's coherence time and frequency.

To compare the pilot overhead performance, three use cases should be investigated. The first use case is when the channel is constant over exactly the same bandwidth and time period as the conventional pilot pattern cluster. In this case, both the APP and the fixed pilot pattern offer the same pilot overhead. The second use case is when the channel is constant over a larger bandwidth or time period than the conventional pilot pattern cluster. In this case, the APP offers better pilot overhead performance since it sends pilots only when the channel changes. The third use case is when the channel is variable over the conventional pilot pattern cluster. In this case, the conventional pilot pattern offers better pilot overhead but at the cost of a BER performance degradation.

In terms of flexibility, APP can be implemented with any architecture while the conventional fixed pilot patterns are limited to a given set of architectures.

In terms of complexity, conventional pilot patterns are mapped once for each MIMO architecture. It is given by (6), where  $n_c$  is the number of  $\delta_f \times \delta_t$  clusters. However, the APP is mapped each time the number of resources in the coherence time and bandwidth changes. That is equivalent to every time the carrier frequency or the bandwidth or the number of subcarriers change. Its complexity is given by (7), where  $n_{cb}$ ,  $n_{csp}$ , and  $n_{cf}$  are respectively the number of times the bandwidth, the number of subcarriers, and the frequency change. Consequently, the APP pilot pattern is more complex.

$$c_{conventional} = o(n_c N_t) \quad (6)$$

$$c_{APP} = o(n_{cb} n_{csp} n_{cf} n_c N_t) \quad (7)$$

### C. APP PERFORMANCE ANALYSIS

APP offers better BER performance than the conventional channel estimation techniques since it guarantees to estimate the channel coefficients within unchanging conditions independently of the channel model and the system's configuration. However, if the number of antennas at the base station exceeds the number of time slots in the coherence time, then we need to use the next subcarrier to send pilots. That leads to the apparition of an error floor during the channel estimation phase.

To analyze this problem, let's take the example of a pilot pattern that considers two subcarriers at the same

coherence bandwidth. At the base station, the initial channel in (8) contains pilots from both subcarriers.

$$H_0 = \begin{pmatrix} h_{k,1}(f_1, t_1) \\ h_{k,2}(f_1, t_2) \\ h_{k,3}(f_1, t_3) \\ h_{k,4}(f_1, t_4) \\ h_{k,5}(f_2, t_1) \\ h_{k,6}(f_2, t_2) \\ h_{k,7}(f_2, t_3) \\ h_{k,8}(f_2, t_4) \end{pmatrix} = \begin{pmatrix} y_k(f_1, t_1)/x_1(f_1, t_1) \\ y_k(f_1, t_2)/x_2(f_1, t_2) \\ y_k(f_1, t_3)/x_3(f_1, t_3) \\ y_k(f_1, t_4)/x_4(f_1, t_4) \\ y_k(f_2, t_1)/x_5(f_2, t_1) \\ y_k(f_2, t_2)/x_6(f_2, t_2) \\ y_k(f_2, t_3)/x_7(f_2, t_3) \\ y_k(f_2, t_4)/x_8(f_2, t_4) \end{pmatrix}, \quad (8)$$

with  $h_{k,i}$  is the channel coefficient corresponding to the  $k^{th}$  antenna of the base station and the  $i^{th}$  antenna of the mobile station,  $f_i$  is the  $i^{th}$  subcarrier,  $t_i$  is the  $i^{th}$  time slot,  $y_k$  is the received signal at the  $k^{th}$  receive antenna of the base station and  $x_i$  is the transmitted symbol from the  $i^{th}$  antenna of the mobile station.

Although the channel is nearly constant, a given channel coefficient  $h_{k,i}(1, t)$  from the first subcarrier and the same coefficient  $h_{k,i}(2, t)$  from the second subcarrier does not exactly have the same value. Therefore, the decoding matrix  $W$  based on the estimated channel  $\hat{H}$  can be written as (9), where  $E$  is a small error value.

$$W(\hat{H}) = W(H) + E, \quad (9)$$

As a result, the estimated signal is expressed by (10).

$$\begin{aligned} \hat{X} &= (W(H) + E)HX + (W(H) + E)N \\ &= W(H)HX + (EHX + W(H)N + EN) \\ &= W(H)HX + N_{tot}, \end{aligned} \quad (10)$$

with  $N_{tot} = EHX + W(H)N + EN$  is the new noise formula. Therefore, the estimation error adds more noise to the post-processing SNR of the estimated channel. Hence, it is decreased compared to the post-processing SNR of a perfect channel.

The bit error probability [37] is given by (11).

$$\begin{aligned} P(PPSNR(\hat{H})) &= N_e N_s Q(\sqrt{(PPSNR(\hat{H})d_{\min}^2)/2}) \\ &= N_e N_s \frac{1}{2\pi} \int_{\sqrt{\frac{PPSNR(\hat{H})d_{\min}^2}{2}}}^{+\infty} \exp\left(\frac{-u^2}{2}\right) du \\ &= N_e N_s \frac{1}{2\pi} \int_{\sqrt{\frac{PPSNR(H)d_{\min}^2}{2}}}^{+\infty} \exp\left(\frac{-u^2}{2}\right) du \\ &\quad + N_e N_s \frac{1}{2\pi} \int_{\sqrt{\frac{PPSNR(\hat{H})d_{\min}^2}{2}}}^{+\infty} \exp\left(\frac{-u^2}{2}\right) du \\ &= \varepsilon + P(PPSNR(H)). \end{aligned} \quad (11)$$

That explains the existence of an error floor  $\varepsilon$ . This analysis is shown in the simulation in Sec.V-B, Fig. 9.

Conventional channel estimation techniques mitigate this phenomenon by handling each line of the initial channel (8) separately with different interpolation's start points [38]. However, this technique is quite complex when it is used with the APP pilot pattern since the channel locations are not known from the beginning. Therefore, the next section suggests a new APP-based channel estimation technique at the base station that solves the error floor's problem automatically without having to deal with each pilot on its own.

#### IV. NEW SHIFTED CHANNEL ESTIMATION

The previous section states that the APP-based channel estimation can encounter an error floor if the number of antennas at the mobile station exceeds the number of OFDM symbols in the coherence time. It is caused by the attribution of the known pilot sequence to different subcarriers on the initial channel matrix before the interpolation phase. Therefore, this paper proposes a new channel estimation (SACE). It solves the error floor's problem while ensuring robust estimation results by adaptively keeping track of any channel model's power profile boundaries.

SACE is composed of three parts (LS channel estimation, BER optimization, and shape correction) as illustrated in Fig. 2.

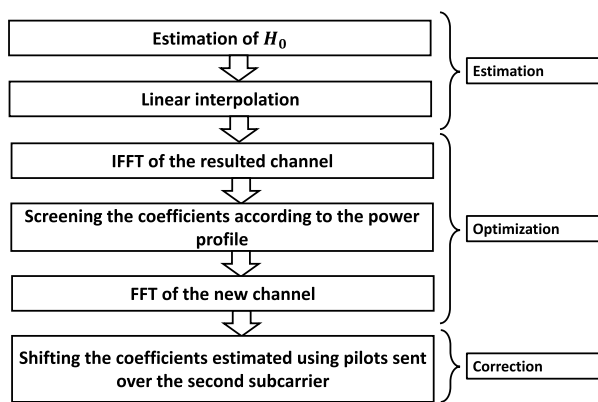


FIGURE 2. SACE scenario.

The estimation part starts at the mobile station. It sends pilots using the APP pilot pattern described in the previous section. Next, at the base station, an initial channel matrix is estimated for each user using the LS channel estimation algorithm as in (8). Then, it is interpolated through all the subcarriers under the same coherence bandwidth.

The optimization part is carried out to decrease the BER. That is done by applying the robust technique in [8] adaptively according to the used channel's power profile. First, the estimated channel's IFFT is computed. After that, the temporal coefficients  $h_n$  are screened following the power profile

corresponding to the adopted channel model as in 15.

$$h_n = \begin{cases} h_n & \text{if } n \in \{l_0, l_1, \dots, l_{L-1}\}. \\ 0 & \text{otherwise.} \end{cases} \quad (12)$$

Hence, if the coefficient belongs to the  $L$  significant paths of the power profile then it is kept as it is or else it is set to zero. Finally, the frequency coefficients are computed again using the fast Fourier transform (FFT) transformation.

The correction part aims to shape the BER curve so that it doesn't meet a constant value. It consists of shifting the coefficients estimated using the pilots of the  $n^{th}$  subcarrier by  $n$  subcarriers in the frequency domain as in Fig. 3.

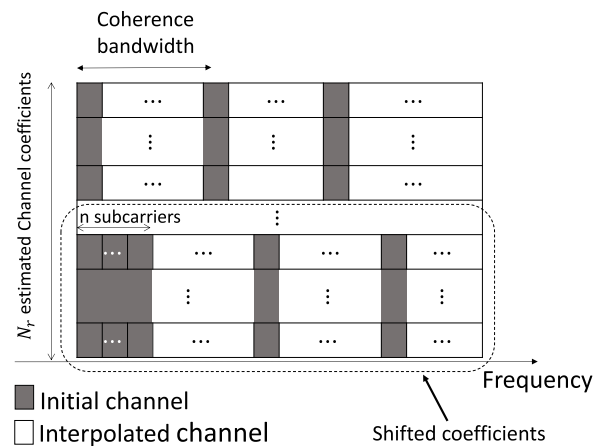


FIGURE 3. Correction part of SACE.

#### V. NUMERICAL STUDY

To study the performances of the APP based on the analysis in the previous sections, we adopted two use cases:  $N_r \leq N_{Tc}$  and  $N_r > N_{Tc}$ .

##### A. USE CASE 1

The main purpose of this study is to compare the BER performance of the APP and the LTE pilot pattern. Matlab simulation of the system described in Sec.II is carried out with the parameters in Table 2.

TABLE 2. Use case 1 system's parameters.

Parameter	Value
Number of subcarriers	512
Number of antennas at the base station	16
Number of antennas at the mobile station	2
Number of users	8
Mobility speed	120 km.h <sup>-1</sup>
Modulation	BPSK
Channel model	SUI4
Estimation technique	LS

This simulation supposes an architecture of one base station with 16 antennas serving 8 users with 2 antennas

each. Moreover, it considers the LTE band 33 i.e. from 1900 to 1920 MHz, since we are using the TDD mode. It adopts  $N = 512$  subcarriers and a mobility speed of  $120 \text{ km.h}^{-1}$ . Furthermore, it adopts the binary phase-shift keying (BPSK) modulation scheme and the LS channel estimation technique.

First, we simulate a scenario where the channel is constant over one subcarrier. In this case, the adopted bandwidth is 20 MHz, then a scenario where the channel is constant over 6 subcarriers. To achieve that, we changed the adopted bandwidth to 4 Mhz.

1) SIMULATION 1: CHANNEL IS CONSTANT OVER ONE SUBCARRIER

The APP applied to the parameters in Table 2 with 20 MHz bandwidth gives the result illustrated in Fig.4. Pilots are inserted in all the subcarriers during two OFDM symbols every period of 32 time slots.

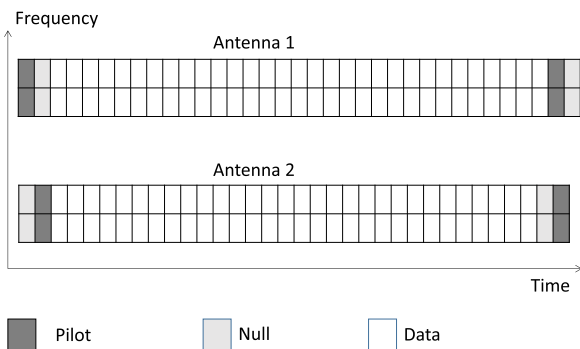


FIGURE 4. APP pilot pattern for SU14 channel model with 20 MHz bandwidth.

Fig.5 shows the result of the BER versus SNR comparison between the APP and the LTE pilot pattern while giving the perfect channel case as a referee.

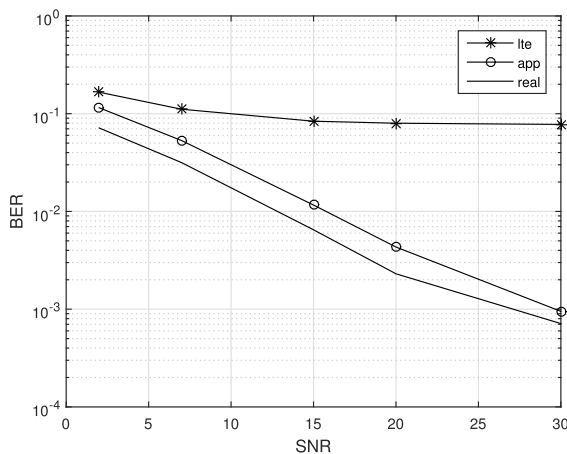


FIGURE 5. BER comparison of APP and LTE pilot pattern with 20 Mhz bandwidth.

The final result shows that the APP reaches a  $BER = 10^{-3}$  for 30 dB while the LTE pilot pattern did not exceed

$BER = 10^{-1}$ . To discuss this result we analyzed the BER and the pilot overhead performances.

a: BER ANALYSIS

After Analyzing the channel’s model and the system’s configuration, the resulted parameters are:  $B_c = 50 \text{ kHz}$ ,  $T_c = 800\mu\text{s}$ ,  $B_s = 49 \text{ kHz}$ ,  $T_s = 25\mu\text{s}$ ,  $\delta_t = 32$ , and  $\delta_f = 1$ . Therefore, to guarantee a correct channel estimation, the known pilots should be sent in all the subcarriers every 32 OFDM symbols. APP meets this requirement since it sends pilots every bloc of one subcarrier and 32 time slots. However, the LTE pilot pattern doesn’t fulfill it since it sends the known pilots every 6 subcarriers and 4 time slots. That explains the fact that the APP offers better performances than the LTE pilot pattern.

b: PILOT OVERHEAD ANALYSIS

Pilot overhead is a crucial criterion for choosing pilot patterns in massive MIMO. Hence, we ought to compare it too to guarantee that the BER performance amelioration won’t cost us any loss in terms of pilot overhead.

Pilot overhead of the LTE pilot pattern applied on this architecture is given by:

$$o_{LTE} = \frac{2}{24} 100 = 8\% \tag{13}$$

Pilot overhead of the APP applied on this architecture is given by:

$$o_{APP} = \frac{2}{32} 100 = 6\% \tag{14}$$

That shows that the APP offers lower pilot overhead than the LTE while ensuring better BER performances.

2) SIMULATION 2: CHANNEL IS CONSTANT OVER SIX SUBCARRIERS

In the last section, we considered a scenario where LTE does not give an optimal BER performance. Hence, in this simulation, we are studying a scenario where the LTE should give an optimal performance (The channel is constant over more than 6 subcarriers and 4 time slots). This is achieved if a total bandwidth of 4 Mhz is used.

The APP applied to this bandwidth is given in Fig.6. Pilots are inserted in two consecutive OFDM symbols, once every 6 subcarriers and 6 time slots.

Fig.7 shows the results of the comparison between APP and LTE pilot pattern with the perfect channel state case as a referee.

The final result shows that the APP and the LTE pilot pattern offer almost the same BER result that reaches  $10^{-3}$  at  $SNR = 30 \text{ dB}$ .

a: BER ANALYSIS

After changing the bandwidth, the new parameters are:  $B_s = 7.8 \text{ kHz}$ ,  $T_s = 128\mu\text{s}$ ,  $\delta_t = 6$ , and  $\delta_f = 6$ . Therefore, to guarantee an optimal BER performance, the estimation

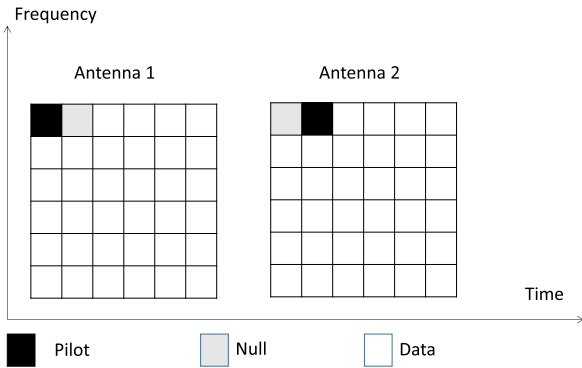


FIGURE 6. APP pilot pattern for SUI4 channel model with 4 MHz bandwidth.

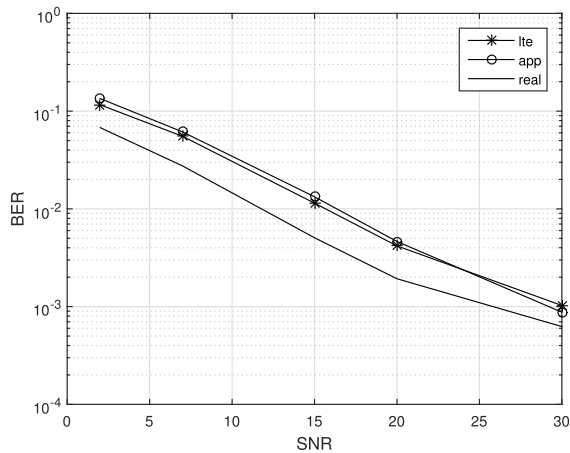


FIGURE 7. BER comparison of APP and LTE pilot pattern with 4 MHz bandwidth.

should restart at least every bloc of  $6 \times 6$  frequency/time resources. This condition is verified by both the APP and the LTE pilot pattern, which explains their BER performances are very close.

**b: PILOT OVERHEAD ANALYSIS**

The pilot overhead of the LTE is the same (8%) since it is fixed for all the adopted bandwidths. However, the APP's pilot mapping changes and is now given by:

$$o_{APP} = \frac{2}{36} 100 = 5\% \tag{15}$$

That shows that in this case, even if the LTE and the APP offer the same BER performance, the APP still grants lower pilot overhead.

**B. USE CASE 2**

The main purpose of this simulation is to investigate the problem of the error floor discussed in Sec.III-B and the BER

TABLE 3. Use case 2 system's parameters.

Parameter	Value
Number of subcarriers	512
Number of antennas at the base station	32
Number of antennas at the mobile station	8
Number of users	4
Frequency bandwidth	100 MHz
Mobility speed	120 km.h <sup>-1</sup>
Modulation	BPSK

performance of the shifted channel estimation technique. It considers the system model described in Sec.II and the configuration in Table 3.

Respecting the fifth generation's specification in [39], this simulation supposes an architecture of 8 antennas at the mobile station and 32 antennas at the base station. Moreover, it considers a bandwidth of 100 MHz in the 28 GHz band divided into  $N = 512$  subcarriers and a mobility speed of 120 km.h<sup>-1</sup>. Furthermore, it adopts the BPSK modulation scheme.

The APP applied to this specification is given by Fig.8. It inserts pilots in two subcarriers and all the OFDM symbols for each bloc of 5 subcarriers.

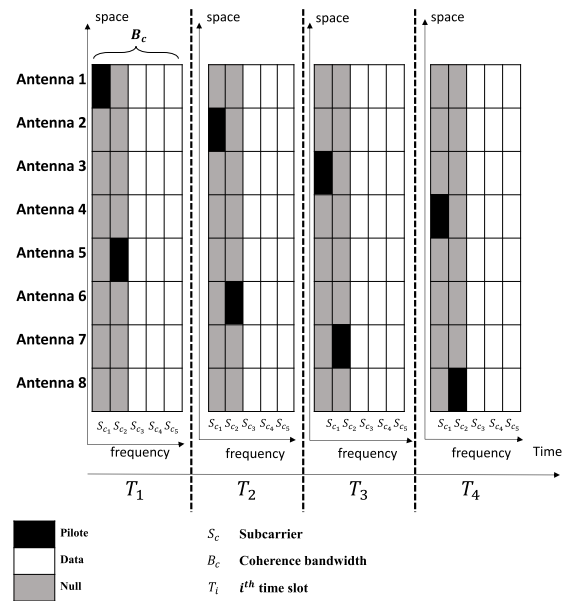


FIGURE 8. APP in the 28 Ghz band.

Fig. 9 illustrates the result of comparing the BER versus SNR of four techniques:

- APP combined with MMSE channel estimation.
- APP-based channel estimation with only the optimization part.
- SACE algorithm.
- Perfect channel.

It shows that the APP faces an error floor of  $BER = 10^{-2}$  if it is combined with conventional channel estimation



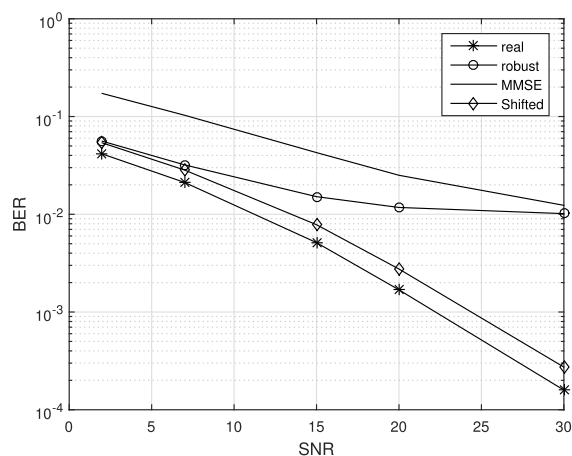


FIGURE 9. BER performances of SACE.

techniques since it uses two subcarriers (instead of 1 in use case 1). That evinces the BER analysis in Sec.III-C.

This error floor disappeared in the case of the SACE algorithm that reaches a  $BER = 10^{-3}$  at  $SNR = 24$  dB. Furthermore, CASE offers an SNR amelioration of 17 dB for  $BER = 10^{-2}$  compared to The APP combined with the conventional MMSE algorithm.

That can be explained by the fact that shifting the coefficients that are estimated using the second subcarrier will lead to their interpolation between the second subcarriers of each coherence bloc. Therefore, the error factor in (9) will no longer exist, and the decoding matrix will be given by (16). Hence, the bit error probability (11) will not face an error floor.

$$W(\hat{H}) = W(H). \quad (16)$$

## VI. CONCLUSION

This paper addresses the pilot pattern optimization issue to ensure its BER optimization. It offers mainly five contributions. First, it proposes an adaptive pilot pattern called APP. Then, it compares it to conventional fixed pilot patterns. Next, it analysis its BER performance. After that, it suggests a new channel estimation called SACE. Finally, it offers a numerical study of the proposed techniques.

The main founded results are:

- APP guarantees a channel estimation within the coherence time and bandwidth independently from the channel model and the system's configuration.
- APP offers equal or better BER than the conventional fixed pilot patterns.
- APP offers equal or lower pilot overhead than conventional pilot patterns without any cost in terms of BER.
- SACE suppresses the error floor caused by the use of more than one subcarrier at the pilot pattern design.
- SACE offers an SNR amelioration of 17dB at  $BER = 10^{-2}$  compared to the MMSE channel estimation.

This APP design considers only the TDD mode. However, several communication technologies are based on the FDD mode. Therefore, further work is needed to use APP combined with the FDD.

## REFERENCES

- [1] H. Bergaoui, Y. Mlayah, F. Tlili, and F. Rouissi, "Switching between diversity and spatial multiplexing in massive MIMO systems," in *Proc. Int. Symp. Ubiquitous Netw.*, Hammamet, Tunisia, 2018, pp. 49–57.
- [2] H. Bergaoui, Y. Mlayah, F. Tlili, and F. Rouissi, "Optimization of a scalable and adaptable diversity/multiplexing trade-Off in 28 GHz systems," in *Proc. 7th Int. Conf. Commun. Netw. (ComNet)*, Hammamet, Tunisia, Nov. 2018, pp. 1–4.
- [3] K. Barner and A. Gonzalo, *Nonlinear Signal and Image Processing: Theory, Methods, and Applications*, 1st ed. Boca Raton, FL, USA: CRC Press, 2004.
- [4] Y. Y. Cheng and J. H. Li, "Subspace-MMSE blind channel estimation for multiuser OFDM with receiver diversity," in *Proc. GLOBECOM*, San Francisco, CA, USA, Dec. 2003, pp. 2295–2299.
- [5] T. Peken, G. Vanhoy, and T. Bose, "Blind channel estimation for massive MIMO," *Analog Integr. Circuits Signal Process.*, vol. 91, no. 2, pp. 257–266, 2017.
- [6] P. Gogoi and K. K. Sarma, "Kalman filter and semi-blind technique-based channel estimation for coded STBC multi-antenna set-ups in faded wireless channels," *Int. J. Inf. Commun. Technol.*, vol. 6, no. 1, pp. 86–108, 2014.
- [7] J. K. Cavers, "An analysis of pilot symbol assisted modulation for Rayleigh fading channels," *IEEE Trans. Veh. Technol.*, vol. 40, no. 4, pp. 686–693, Nov. 1991.
- [8] Y. Mlayah, F. Tlili, F. Rouissi, I. Ouachani, and A. Ghzel, "Performance evaluation and analysis of switching algorithms in MIMO-OFDM system with ideal and non-ideal CSI," *Int. J. Commun., Netw. Syst. Sci.*, vol. 3, no. 12, pp. 945–953, 2010.
- [9] Y. Shen and E. Martinez. (2006). *Channel Estimation in OFDM Systems*. Freescale Semiconductor. Accessed: May 15, 2021. [Online]. Available: <https://www.academia.edu/>
- [10] R. K. Kahlon, G. S. Walia, and A. Sheetal, "Channel estimation techniques in MIMO-OFDM systems—review article," *Int. J. Adv. Res. Comput. Commun. Eng.*, vol. 4, no. 5, pp. 637–642, May 2015.
- [11] E. G. Larsson, O. Edfors, F. Tufvesson, and T. L. Marzetta, "Massive MIMO for next generation wireless systems," *IEEE Commun. Mag.*, vol. 52, no. 2, pp. 186–195, Feb. 2014.
- [12] X. Zhu, Z. Wang, L. Dai, and C. Qian, "Smart pilot assignment for massive MIMO," *IEEE Commun. Lett.*, vol. 19, no. 9, pp. 1644–1647, Sep. 2015.
- [13] N. Akbar, S. Yan, N. Yang, and J. Yuan, "Location-aware pilot allocation in multicell multiuser massive MIMO networks," *IEEE Trans. Veh. Technol.*, vol. 67, no. 8, pp. 7774–7778, Aug. 2018.
- [14] X. Luo, X. Zhang, P. Cai, and H. Qian, "Aligning power in multiple domains for pilot decontamination in massive MIMO," *IEEE Trans. Wireless Commun.*, vol. 16, no. 12, pp. 7919–7935, Dec. 2017.
- [15] P. Liu, S. Jin, T. Jiang, Q. Zhang, and M. Matthaiou, "Pilot power allocation through user grouping in multi-cell massive MIMO systems," *IEEE Trans. Commun.*, vol. 65, no. 4, pp. 1561–1574, Apr. 2017.
- [16] R. M. Rao, V. Marojevic, and J. H. Reed, "Rate-maximizing OFDM pilot patterns for UAV communications in nonstationary A2G channels," in *Proc. VTC-Fall*, Chicago, IL, USA, Aug. 2018, pp. 1–5.
- [17] R. M. Rao, V. Marojevic, and J. H. Reed, "Adaptive pilot patterns for CA-OFDM systems in nonstationary wireless channels," *IEEE Trans. Veh. Technol.*, vol. 67, no. 2, pp. 1231–1244, Feb. 2018.
- [18] Y. Nie, X. Yu, and Z. Yang, "Deterministic pilot pattern allocation optimization for sparse channel estimation based on CS theory in OFDM system," *EURASIP J. Wireless Commun. Netw.*, vol. 2019, no. 1, pp. 1–8, Dec. 2019.
- [19] I. Khan, M. Singh, and D. Singh, "Compressive sensing-based sparsity adaptive channel estimation for 5G massive MIMO systems," *Appl. Sci.*, vol. 8, no. 5, p. 754, May 2018.
- [20] J.-Y. Choi, H.-S. Jo, C. Mun, and J.-G. Yook, "Preamble-based adaptive channel estimation for IEEE 802.11p," *Sensors*, vol. 19, no. 13, p. 2971, Jul. 2019.
- [21] P. Su and Y. Wang, "Channel estimation in massive MIMO systems using a modified Bayes-GMM method," *Wireless Pers. Commun.*, vol. 107, no. 4, pp. 1521–1536, Aug. 2019.

- [22] *Physical Channels and Modulation*, Standard 3GPP TS 38.211, Version 15.2.0, Release 15, 2018.
- [23] *LTE Evolved Universal Terrestrial Radio Access (E-UTRA); Physical Channels and Modulation*, Standard 3GPP TS 36.211, Version 14.2.0, Release 14, 2017.
- [24] *Standard for Local and Metropolitan Area Networks. Part 16: Air Interface for Fixed and Mobile Broadband Wireless Access Systems, Amendment 2: Physical and Medium Access Control Layers for Combined Fixed and Mobile Operation in Licensed Bands and Corrigendum*, Standard IEEE 802.16e-2005, 2006.
- [25] E. Björnson, E. G. Larsson, and T. L. Marzetta, "Massive MIMO: Ten myths and one critical question," *IEEE Commun. Mag.*, vol. 54, no. 2, pp. 114–123, Feb. 2016.
- [26] J. Jose, A. Ashikhmin, P. Whiting, and S. Vishwanath, "Channel estimation and linear precoding in multiuser multiple-antenna TDD systems," *IEEE Trans. Veh. Technol.*, vol. 60, no. 5, pp. 2102–2116, Jun. 2011.
- [27] T. L. Marzetta, "Noncooperative cellular wireless with unlimited numbers of base station antennas," *IEEE Trans. Wireless Commun.*, vol. 9, no. 11, pp. 3590–3600, Nov. 2010.
- [28] Z. Gao, L. Dai, Z. Wang, and S. Chen, "Spatially common sparsity based adaptive channel estimation and feedback for FDD massive MIMO," *IEEE Trans. Signal Process.*, vol. 63, no. 23, pp. 6169–6183, Dec. 2015.
- [29] X. Rao and V. K. N. Lau, "Distributed compressive CSIT estimation and feedback for FDD multi-user massive MIMO systems," *IEEE Trans. Signal Process.*, vol. 62, no. 12, pp. 3261–3271, 2014.
- [30] E. Karani, M. Beheshti, and M. S. Fazel, "Beyond-sparsity-based doubly selective channel estimation for high-mobility multiuser MIMO-OFDM systems," *Trans. Emerg. Telecommun. Technol.*, vol. 30, no. 12, p. e3636, Dec. 2019.
- [31] V. C. Rodrigues, J. C. Marinello, and T. Abrão, "Exponential spatial correlation with large-scale fading variations in massive MIMO channel estimation," *Trans. Emerg. Telecommun. Technol.*, vol. 30, no. 5, p. e3563, May 2019.
- [32] K. Upadhyaya, "Channel estimation in large-scale multi-antenna systems for 5G and beyond—Novel pilot structures and algorithms," Ph.D. dissertation, Dept. Signal Process. Acoust., Aalto Univ., Espoo, Finland, 2016.
- [33] M.-H. Hsieh and C.-H. Wei, "Channel estimation for OFDM systems based on comb-type pilot arrangement in frequency selective fading channels," *IEEE Trans. Consum. Electron.*, vol. 44, no. 1, pp. 217–225, Feb. 1998.
- [34] F. Rusek, D. Persson, B. K. Lau, E. G. Larsson, T. L. Marzetta, and F. Tufvesson, "Scaling up MIMO: Opportunities and challenges with very large arrays," *IEEE Signal Process. Mag.*, vol. 30, no. 1, pp. 40–60, Jan. 2013.
- [35] J. Ma and L. Ping, "Data-aided channel estimation in large antenna systems," *IEEE Trans. Signal Process.*, vol. 62, no. 12, pp. 3111–3124, 2014.
- [36] H. Q. Ngo and E. G. Larsson, "EVD-based channel estimation in multi-cell multiuser MIMO systems with very large antenna arrays," in *Proc. ICASSP*, Kyoto, Japan, 2012, pp. 3249–3252.
- [37] Y. Mlayah, "Optimization of the performances offered by MIMO technology for wireless links (applied to WIMAX IEEE 802.16e)(Optimisation de performances offertes par la technologie MIMO pour des liaisons sans fil (application à la norme WIMAX mobile IEEE 802.16e))," Ph.D. dissertation, Dept. ITC, Carth. Univ., Tunis, Tunisia, 2012.
- [38] *Evolved Universal Terrestrial Radio Access (E-UTRA); Base Station (BS) Conformance Testing. 3rd Generation Partnership Project; Technical Specification Group Radio Access Network*, Standard 3GPP TS 36.141, 2017.
- [39] M. SERIES. (2015). *IMT Vision—Framework and Overall Objectives of the Future Development of IMT for 2020 and Beyond*. [Online]. Available: <https://www.itu.int/> Accessed: Mar. 28, 2021.



**HALIMA BERGAOUI** was born in Tunisia, in 1992. She received the Diploma degree in engineering from the National Institute of Applied Science and Technology (INSAT). She is currently pursuing the Ph.D. degree in information and communications technology. She is affiliated with the Innovative and Green Communications Systems Laboratory (GRESKOM), Higher School of Communication of Tunis.



**YOSRA MLAYEH** was born in Tunisia. She received the Diploma degree in national engineering and the Ph.D. degree in information and communications technology from the Higher School of Communication of Tunis. She is currently affiliated with the GRESKOM Laboratory.



**FETHI TLILI** is currently a Tunisian Professor in the Higher School of Communication of Tunis. He is also affiliated with the GRESKOM Laboratory.

• • •